Spectrochimica Acta Part A: Molecular and Biomolecular Spectroscopy 109 (2013) 110–115

Contents lists available at SciVerse ScienceDirect

Spectrochimica Acta Part A: Molecular and Biomolecular Spectroscopy

journal homepage: www.elsevier.com/locate/saa

Signal amplification aptamer biosensor for thrombin based on a glassy carbon electrode modified with graphene, quantum dots and gold nanoparticles

Lingling Xie *, Liqin You, Xiaoyu Cao *

School of Chemistry and Chemical Engineering, Henan University of Technology, Zhengzhou 450001, China

HIGHLIGHTS

- A electrogenerated chemiluminescence assay for thrombin is designed.
- CdSe/ZnS quantum dots are served as ECL label.
- Low surface coverage of gold nanoparticles is involved to improved sensitivity.
- The sensing system is based on the utilization of aptamer as the probes.

GRAPHICAL ABSTRACT

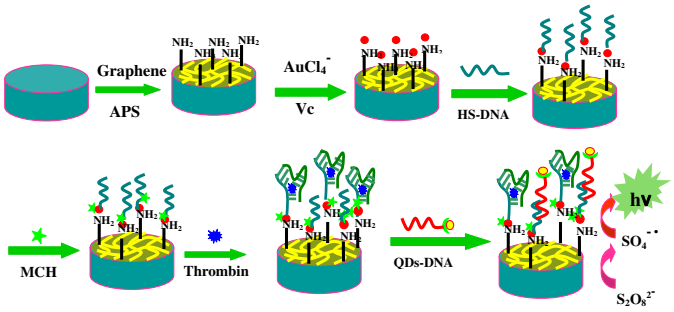

ARTICLE INFO

Article history:
Received 13 December 2012
Received in revised form 25 January 2013
Accepted 2 February 2013
Available online 21 February 2013

Keywords:
Electrogenerated chemiluminescence
CdSe/ZnS quantum dots
Aptamer
Thrombin
Gold nanoparticles

ABSTRACT

A novel electrogenerated chemiluminescence (ECL) assay for sensitive determination of thrombin is designed employing CdSe/ZnS quantum dots served as an ECL label. This ECL sensor is fabricated on graphene modified glassy carbon electrode which is then covered with a low surface coverage of gold nanoparticles (AuNPs). An aptamer is used to selectively recognize the target. The thiol-terminated aptamer is first immobilized on AuNPs/graphene modified electrode, and then thrombin is imported to form the aptamer–thrombin complexes. After blocking the nonspecifically bound oligonucleotides with MCH solution, another CdSe/ZnS quantum dots modified aptamer is hybridized with the free thiol-terminated aptamer to form a DNA complexe. A decreased ECL signal is observed upon recognition of the target thrombin. The integrated ECL intensity versus the concentration of thrombin is linear in the range from 0.01 to 50 nM. The detection limit is 10 fM. The present aptasensor also exhibits excellent selectivity, stability and reusability. This sensing system can provide a promising label-free model for aptamer-based compounds sensitive detection.

Introduction

Aptamers are single stranded DNA molecules or RNA that selectively bind to various target molecules with high affinity, such as small molecules, proteins and drugs [1–5]. Compared to traditional molecular recognition system, aptamers have a lot of advantages in terms of the simplicity of synthesis. Aptamers can be stored stable for a long term, ease of labeling, excellent stability, wide applicability, and high sensitivity. It is regarded as the ideal recognition elements for a broad range of biosensing applications, such as optical, electrochemical and electrogenerated chemiluminescence (ECL) biosensors [6–10].

In aptamer-based assay, highly luminescent semiconductor nanocrystals, often referred to as quantum dots (QDs), have received tremendous attention for their possible luminescent applications in aqueous solution [11,12]. With size tunable narrow emission spectra and broad excitation spectra, they have been widely used as multicolored luminescent probes, biological labels and bioimaging [13,14].

Gold nanoparticles (AuNPs) have been widely used because of the excellent properties, such as high biocompatibility, distinctive

* Corresponding authors. Tel./fax: +86 371 67756718.
E-mail addresses: linglingxie@haut.edu.cn (L. Xie), caoxy@haut.edu.cn (X. Cao).

1386-1425/$ - see front matter © 2013 Elsevier B.V. All rights reserved.
http://dx.doi.org/10.1016/j.saa.2013.02.017

size-related electronic and optical behavior, good conductivity and high catalytic activity [15–17]. However, large size or high surface coverage of AuNPs may exhibit high and potential-dependent background current in aqueous solution because of their high capacitive current and complex surface redox reactions. The modification of electrodes with a low surface coverage of AuNPs will allow high electrocatalytic activities along with low background current. This is helpful to achieve high signal-to-background ratios (i.e., low detection limits). Moreover, the use of minimal Au may reduce the cost of electrochemical sensors.

The objective of this work is to develop a novel ECL assay for thrombin detection with quantum dots CdSe/ZnS served as an ECL label. For improving the detection sensitivity, graphene is used in the construction of the biosensor. Graphene has stimulated intense research interest because of its unique physical and chemical properties, such as high surface area, high electrical conductivity, good chemical stability and strong mechanical strength [18–20]. In addition, the ease of material processing, low cost of synthesis, and ability to make composite materials make it an attractive candidate for fabricating various functional devices, such as electrodes, sensors, photovoltaics and photodetectors [21–24]. For further signal amplification and introduction of aptamer, a low surface coverage of AuNPs was *in situ* reduced on glassy carbon electrode (GCE). The thiol-terminated aptamer is then immobilized on AuNPs/graphene modified electrode, and then thrombin was imported to form the aptamer–thrombin complexes. After blocking the nonspecifically bound oligonucleotides with MCH solution, another CdSe/ZnS quantum dots modified aptamer was hybridized with the free thiol-terminated aptamer to form a DNA complexe. A decreased ECL signal was observed upon recognition of the target thrombin and therefore could be used to detect thrombin. The developed ECL assay was specific and sensitive, and it could be applied for sensitive detection of other molecules only needing change of the aptamer.

Experimental

Chemicals and materials

Labeled DNA oligonucleotides were synthesized by Shanghai Sangon Biotechnology Co., Ltd. (Shanghai, China, www.sangon.com), purified by C_{18} HPLC and PAGE, confirmed by mass spectrometry and used as received. The sequences of two oligomers employed were given below: 5′-HS-$(CH_2)_6$-AGTCCGTGGT AGGGCAGGTTGGGGTGACT-3′ (HS-DNA); 5′-biotin-GGTTGGTGTG GTTGG-3′ (Biotin-DNA). 6-mercapto-1-hexanol (MCH), Adenosine triphosphate (ATP), lysozyme, fibrinogen, bovine serum albumin (BSA), thrombin, immunoglobulin (IgG), and 3-aminopropyl triethylene silane (APS) were purchased from Sigma–Aldrich (Saint Louis, MO, USA, http://www.sigmaaldrich.com). Avidin-QDs (with a CdSe/ZnS core–shell structure about 10 nm) were obtained from Wuhan Jiayuan Quantum Dots Co., Ltd. (Wuhan, China, www.qds.net.cn) with a prime concentration of 1.10 μM. 0.1 M of phosphate-buffered saline (PBS) with various pH values was prepared by mixing the stock solutions of NaH_2PO_4 and Na_2HPO_4 and then adjusting the pH with 0.1 M NaOH and H_3PO_4. The buffer solution (pH 7.4) for oligonucleotides contained 100 mmol L^{-1} $Na_2HPO_4 + NaH_2PO_4$ and 5 mmol L^{-1} $MgCl_2$. The electrolyte for ECL measurement was 5 mL PBS solution containing 0.1 mol L^{-1} $K_2S_2O_8$ and 0.1 mol L^{-1} KCl. Solution contained 0.1 mol L^{-1} KCl and 2 mmol L^{-1} $[Fe(CN)_6]^{3-}/[Fe(CN)_6]^{4-}$ was used for electrochemical impedance spectroscopy (EIS) characterization. Millipore ultrapure water (resistivity $\geqslant$ 18.2 MΩ) was used throughout the experiment. All other reagents were of analytical reagent grade and used without further purification.

Apparatus

The ECL emission was detected using a model MPI-A ECL analyzer (Xi'an Remex Analysis Instrument Co., Ltd., Xi'An, China, http://www.xaremex.com). The spectral width of the photomultiplier tube (PMT) was 200–800 nm, and the voltage of the PMT was 500–800 V in the detection process. The scanning electron microscopy image was obtained using JSM-5800 scanning microscope (JEOL. Ltd., Tokyo, Japan http://www.jeol.com).

Preparation of modified electrode

Graphene oxide (GO) was prepared from graphite powder by the modified Hummers method [18]. In a typical process, 5 g graphite was slowly added into a stirred mixture of concentrated H_2SO_4 (87.5 mL) and fuming HNO_3 (45 mL) cooling in an ice-water bath. $KClO_3$ (55 g) was then added slowly in above mixture. The mixture was kept stirring for 96 h at room temperature. Then the slurry was poured into water and filtered to obtain graphite oxide. After dried at 80 °C, graphite oxide (0.5 g) was exfoliated in de-ionized water (500 mL) with ultrasonic treatment to form a colloidal graphene oxide suspension (1 mg mL^{-1}). To get graphene, chemical reduction of the suspension of GO was carried out with hydrazine monohydrate for 24 h at 80 °C. The final product was isolated by filtration, and rinsed thoroughly with deionized water and ethanol. Then the product was dried in vacuum and graphene was obtained.

The GCE (3 mm in diameter) was polished carefully with 0.3 and 0.05 μm alumina slurry, and sonicated in acetone, ethanol, 0.5 M NaOH, and ultrapure water, respectively. Graphene (1 mg) was dispersed in 10 mL water and the mixture was sonicated for 30 min to obtain a homogeneous suspension. Next, with a microinjector, 10 μL of the mixture was dropped on the surface of GCE. The graphene modified electrode was then immersed in APS solution (2%, v/v) for 0.5 h to introduce the amine functional groups monolayer. The modified electrode was rinsed several times with water. Then the electrode was dried under a stream of nitrogen. Prepared in this way, the substrate surface was covered with positively charged APS that readily adsorbed $HAuCl_4$ with negative charge. The functionalized electrode with amine was immersed into 1 mM $HAuCl_4$ solution for 30 min at 37 °C. The $AuCl_4^-$ ions were electrostatically bound to protonated amine groups. After the electrode was modified, it was thoroughly rinsed with water, the $AuCl_4^-$ ions at the electrode was reduced by using 0.5 mM ascorbic acid for 2 h. Then the modified electrode was washed with water and dried at 50 °C for 20 min. To increase the size of AuNPs (for comparison), the electrode was treated in an aqueous solution containing 0.3 mM $HAuCl_4$ and 0.3 mM NH_4OH (30%, v%).

The HS-DNA was dissolved in 10 mM PBS solution (0.1 M NaCl, 5 mM $MgCl_2$, 1 mM TCEP, pH 7.4) to a final concentration of 2 μM. The modified electrode was immersed into this solution for 3 h to adsorb HS-DNA on the AuNPs. The electrode was then washed with PBS (pH 7.4) and subsequently immersed in 1 mM MCH solution (10 mM PBS, 1 M NaCl, pH 7.4) for 2 h to displace the nonspecifically bound oligonucleotides. The resulting electrode was again washed with PBS and used as ECL biosensor. The construction of the ECL biosensor was shown in Scheme 1.

Electrogenerated chemiluminescence detection

The Avidin-QDs solution was diluted 50 times with 0.1 M PBS (pH 7.4). Then the same volume of 10 μM Biotin-DNA was added and incubated at 37 °C for 1.5 h to form the QDs and DNA complex QDs-DNA. The biosensor was immersed in thrombin solution for 1 h, and then washed with PBS. After dried with a stream of N_2, the electrode was immediately covered with 20 μL QDs-DNA for

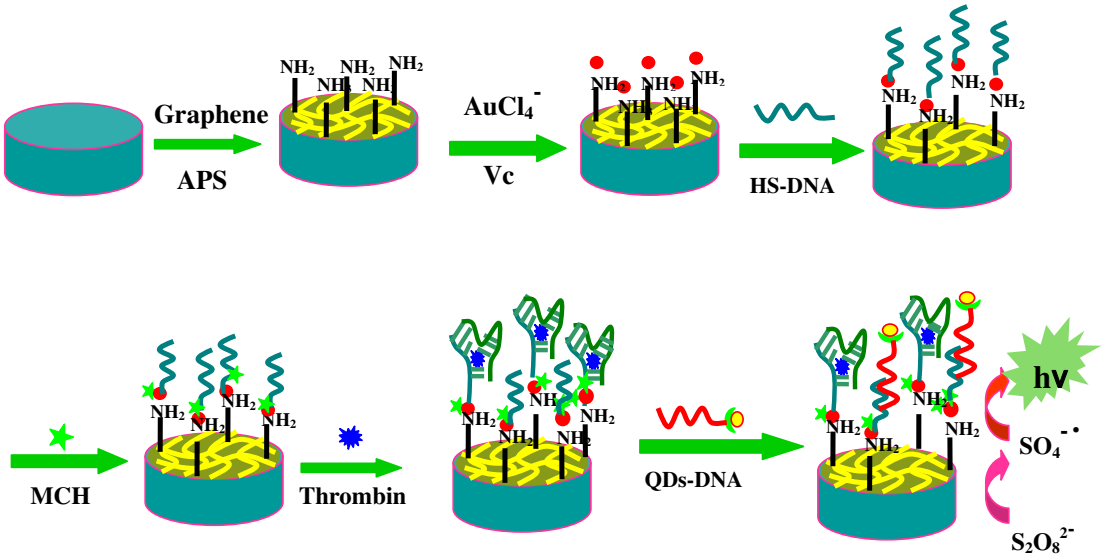

Scheme 1. Schematic diagram for the ECL biosensor fabrication.

another 2 h. All above incubation steps were carried out at 37 °C. The measurement of thrombin was performed with cyclic voltammogram at a potential ranging from 0.0 V to −1.7 V at a scan rate of 100 mV s^{-1} with a conventional three-electrode system. The modified electrode, a platinum wire, and an Ag/AgCl (saturate KCl) electrode were used as working electrode, counter electrode and reference electrode, respectively.

Results and discussion

In situ reduction of gold nanoparticles

AuNPs have been recognized as a versatile and efficient template for the immobilization of biomolecules. They could not only act as "electronic wires" to enhance the electron transfer between redox centers and electrode, but also as catalysts to increase electrochemical reaction of electroactive species [25,26]. In this work, in order to improve the detection sensitivity, low surface coverage of AuNPs was reduced *in situ* on electrode with ascorbic acid after the substrate surface was covered with positively charged APS. Fig. 1 shows the SEM images of AuNPs. Some bright spots were observed in Fig. 1a. This might be associated with AuNPs formation on the substrate surface. The AuNPs were very small, and it could not be clearly recognized in the SEM images. The AuNPs were then used as seeds to induce the further growing of AuNPs. The substrate covered with the small AuNPs were then immersed into an aqueous solution containing 0.3 mM $HAuCl_4$ and 0.3 mM NH_4OH (30%, v%) for 10 min. As shown in Fig. 1b, the formation of large AuNPs indicated the presence of small and low-coverage AuNPs on the electrode. Fig. 2 showed that the ECL intensity was obviously increased on the low surface coverage of AuNPs modified GCE compared to the large AuNPs.

Electrochemical impedance spectroscopy

Electrochemical impedance spectroscopy (EIS) provides detailed information on the change of the surface property of modified electrodes for each modification process. The typical impedance spectrum that presents in the form of the Nyquist plot includes a semicircle portion at higher frequencies corresponding to the electron-transfer limited process and a linear part at lower frequency range representing the diffusion limited process. The semicircle diameter in the impedance spectrum is equal to the electron-transfer resistance (Ret) which reflects the electron transfer kinetics of the redox probe at the electrode. Fig. 3 shows the impedance spectra corresponding to the stepwise modification processes. It was observed that the EIS of the bare GCE displayed an electron-transfer resistance of about 78 Ω (Fig. 3a). After graphene and APS were coated on the GCE, the Ret of the resultant APS/graphene/GCE obviously decreased to 58 Ω (Fig. 3b), indicating

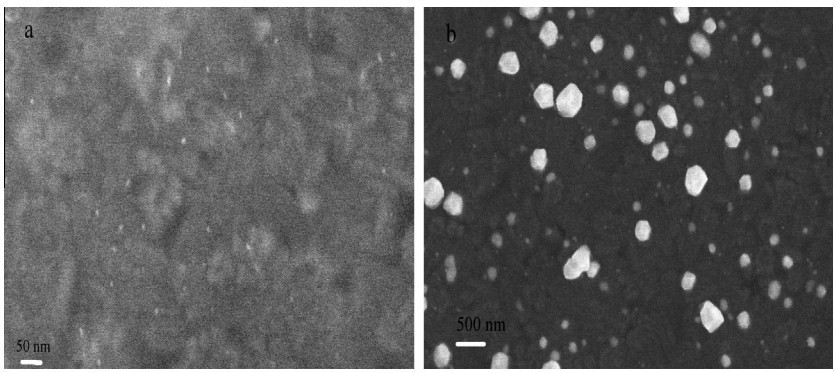

Fig. 1. SEM images of: (a) AuNPs modified electrodes and (b) after (a) was treated in an aqueous solution containing 0.3 mM $HAuCl_4$ and 0.3 mM NH_4OH (30%, v%).

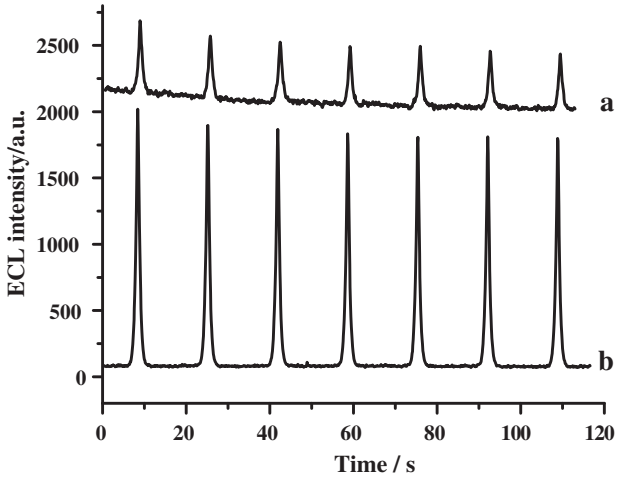

Fig. 2. The ECL of: (a) biosensor modified with the *in situ* production of low surface coverage of AuNPs and (b) biosensor modified with AuNPs.

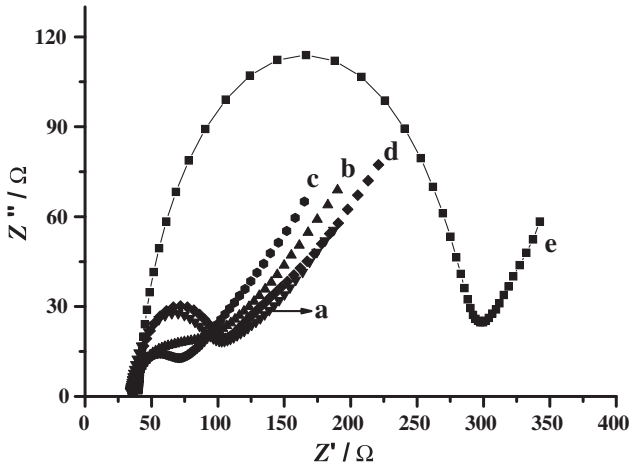

Fig. 3. EIS of the ECL biosensor at different stages in 0.1 M KCl and 2 mM $Fe(CN)_6^{4-/3-}$: (a) Bare GCE, (b) APS/graphene/GCE, (c) AuNPs/APS/graphene/GCE, (d) HS-DNA/AuNPs/APS/graphene/GCE, and (e) Thrombin/HS-DNA/AuNPs/APS/graphene/GCE.

good conductivity of graphene. After AuNPs was immobilized on the electrode, the Ret of the modified electrode obviously decreased to 47 Ω (Fig. 3c), indicating that AuNPs acted as high electron relay for shuttling electron between the electrochemical probe and the electrode. After the immobilization of HS-DNA, an obvious increase of semicircle part of the impedance spectrum appeared, and the Ret increased to 76 Ω (Fig. 3d). Because the negative charge of DNA hindered $[Fe(CN)_6]^{4-/3-}$ from reaching to the electrode surface, the increase in electron transfer resistance indicated that the HS-DNA was successfully immobilized on the electrode. When thrombin was bound on the modified electrode, the electron-transfer resistance greatly increased to 273 Ω (Fig. 3e). This resistance enlargement could be attributed to the fact that the resistive hydrophobic layer of thrombin molecules insulated the conductive support and perturbed the interfacial electron transfer between the electrode and the electroactive species in solution.

Electrogenerated chemiluminescence behavior

As shown in Fig. 4, the ECL signals of the electrodes (including Thrombin/HS-DNA/AuNPs/APS/graphene/GCE, HS-DNA/AuNPs/APS/graphene/GCE, AuNPs/APS/graphene/GCE, APS/graphene/GCE), which was in the absence of QDs, were very low. After QDs-Avidin-DNA were added to form DNA complex on the modified electrode, the ECL intensity increased greatly (curve a). This indicated the ECL signal was caused by QDs. When the negative potential scan was performed, the QDs immobilized on the electrode surface and $S_2O_8^{2-}$ in the aqueous solution could be reduced to nanocrystal species ($QD^{\bullet-}$) and $SO_4^{\bullet-}$, respectively. Then $QD^{\bullet-}$ reacted with $SO_4^{\bullet-}$ to produce excited state QD^* to emit light. In this work, the thrombin aptamer was attached to AuNPs via alkane thiol self-assembled monolayer. Target induced association of the two DNAs (HS-DNA and QDs-DNA) thus increases the concentration of QDs at the electrode surface, which therefore increased the intensity of ECL.

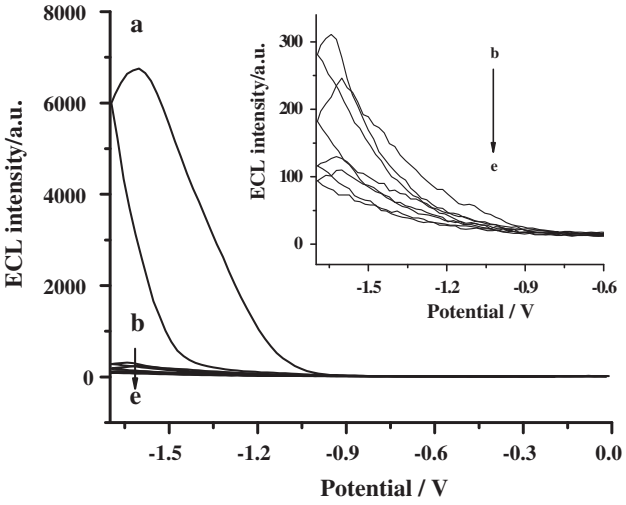

Fig. 4. ECL intensity versus potential: (a) QDs-Avidin-DNA/Thrombin/HS-DNA/AuNPs/APS/graphene/GCE, (b) Thrombin/HS-DNA/AuNPs/APS/graphene/GCE, (c) HS-DNA/AuNPs/APS/graphene/GCE, (d) AuNPs/APS/graphene/GCE, and (e) APS/graphene/GCE. The inset is the amplification form of curve (b–e).

Optimization

The effect of the reaction time between QDs-DNA and HS-DNA was investigated. With time increased from 0 to 2 h, the ECL signal rapidly increased. The ECL response reached a steady state after 2 h, indicating the contracting species were almost transferred to the complexes. Therefore, 2 h of incubation time was used in the subsequent work.

The influence of the $K_2S_2O_8$ concentration on the ECL intensity was also discussed. Different $K_2S_2O_8$ concentrations (0.05–0.5 M) were employed and the ECL intensity kept almost unchanged. This indicated that the coreactant was adequate for the ECL consumption during the measurement. Therefore, 0.1 M coreactant $K_2S_2O_8$ was selected.

Determination of thrombin

The presence of thrombin at different concentrations led to different ECL intensity, depending on the amount of the free HS-DNA on the modified electrode, which subsequently reacted with QDs-DNA. In order to evaluate the performance of the present ECL biosensor, a series of thrombin solutions were tested. The difference in ECL intensity was used to evaluate the response to thrombin. The ECL intensity decreased with the increase of thrombin concentration until reached a maximal value at 50 nM thrombin. As shown in Fig. 5, the biosensor showed linear relationship between the ECL intensity and the logarithm of the thrombin concentration in the range from 0.01 nM to 50 nM. The linear regression equations

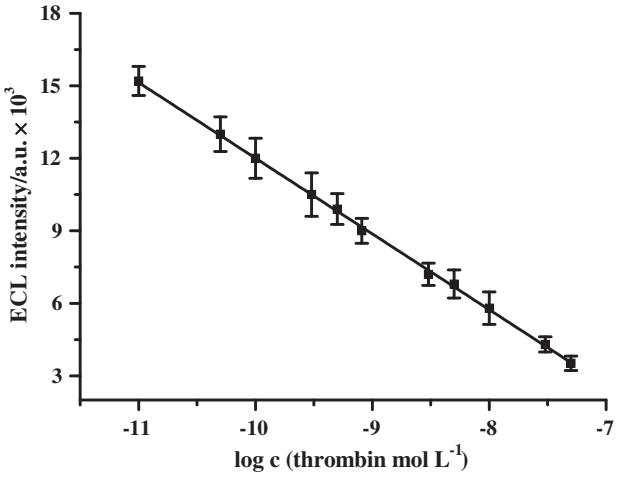

Fig. 5. The ECL intensity of the ECL biosensor with different thrombin concentrations.

were $Y = -3.133 \log X - 19.327$, with correlation coefficients of $R = 0.996$. Three repetitions of each standard thrombin solution were carried out to evaluate the reproducibility and precision of the method. The results were reflected by the error bars in Fig. 5. The detection limit was 10 fM based on a signal-to-noise ratio of 3. This indicated that the ECL sensor was highly sensitive and reproductive.

Precision, selectivity, and stability

The precision of the ECL sensors was investigated by using the variation coefficients of intra- and inter-assays. The intra-assay precision of the analytical method was evaluated by analyzing five concentration levels of thrombin for three times per run. The variation coefficients of intra-assay were 3.2%, 3.6%, 2.9%, 3.1% and 4.3% at 0.05, 0.1, 0.5, 1 and 30 nM of thrombin, respectively. Similarly, the variation coefficients of the inter-assay were 4.2%, 5.1%, 5.8%, 5.4%, and 5.9% at 0.05, 0.1, 0.5, 1 and 30 nM of thrombin, respectively. Therefore, the precision and reproducibility of the ECL sensors was acceptable.

Selectivity is one of the potential advantages of using aptamer as recognition elements. To monitor the differences in response of the sensor to interference degree or crossing recognition level, some compounds including ATP, IgG, lysozyme, fibrinogen and BSA were used to evaluate the selectivity of the sensor. The sensor was separately exposed to two types of 1 nM thrombin: one with interference and the other without. The results were shown in Table 1, which indicated that the selectivity of the sensor was acceptable within experimental error.

Table 1
Interference studies with the ECL biosensor.

Interferent	ATP	Lysozyme	Fibrinogen	IgG	BSA
ECL intensity (a.u.)[a]	8875				
ECL intensity (a.u.)[b]	8810	8821	8912	8823	8790
Difference of ECL intensity[c] (%)	−0.73	−0.61	0.42	−0.59	−0.96

[a] ECL intensity after biosensor incubated with 1 nM thrombin without the interference.
[b] ECL intensity after biosensor incubated with 1 nM thrombin with the interference.
[c] Difference of ECL intensity ratio = (ECL intensity (a.u.)[b] – ECL intensity (a.u.)[a])/ECL intensity (a.u.)[a].

Table 2
Recovery of thrombin assay in human serum sample ($n = 3$).

Samples	Added (nM)	Found (nM)	Recovery (%)	R.S.D. (%)
1	0.05	0.048	96.0	3.2
2	0.1	0.093	93.0	2.4
3	1	1.045	104.5	2.1
4	5	5.19	103.8	2.5
5	10	9.71	97.1	3.8

The stability of the sensor was examined. When the sensor was stored at 4 °C and measured every day, the ECL signal of the conserved ECL sensor decreased only 2.5% and 3.2% of its initial response after storing for 15 and 30 days, respectively. Obviously, the resulting aptamer based ECL sensor achieved sufficient stability.

Analytical application

The practical applicability of the biosensor was investigated by detecting thrombin in human serum sample. The standard addition method was employed. Herein, a series of samples were prepared by adding thrombin of different concentrations to human serum. The analytical results for thrombin were shown in Table 2. From Table 2 we could see that the recovery (between 93.0% and 104.5%) and relative standard deviation values (between 2.1% and 3.8%) were acceptable, which clearly indicated the potentiality of this biosensor for thrombin detection in real biological samples.

Conclusion

In this work, a novel, label free assay based on aptamer was developed with high sensitivity and specificity for a big molecule as an example of thrombin. Quantum dots CdSe/ZnS was employed as sensing probe. A low surface coverage of gold nanoparticles *in situ* produced on the graphene modified GCE significantly improved ECL signal. The ECL biosensor, combined both highly selective thrombin–binding aptamer and highly sensitive signal amplification assay, has demonstrated the success and robustness in the detection of trace amount of thrombin. The present ECL biosensor design may offer several unique features such as high sensitivity and high selectivity. In addition, this aptamer sensing strategy based on aptamer recognition and low surface coverage of gold nanoparticles and graphene amplification was versatile and had great potential in the construction of aptamer based biosensors for the detection of various molecules.

References

[1] A.D. Ellington, J.W. Szostak, Nature 346 (1990) 818–822.
[2] C. Tuerk, L. Gold, Science 249 (1990) 505–510.
[3] X. Zuo, S. Song, J. Zhang, D. Pan, L. Wang, C. Fan, J. Am. Chem. Soc. 129 (2007) 1042–1043.
[4] R.Y. Lai, K.W. Plaxco, A.J. Heeger, Anal. Chem. 79 (2007) 229–233.
[5] G.S. Bang, S.Y. Cho, N. Lee, B.R. Lee, J.H. Kim, B.G. Kim, Biosensors. Bioelectron. 39 (2013) 44–50.
[6] J. Liu, Y. Lu, Angew. Chem. 118 (2006) 96–100.
[7] E. Heyduk, T. Heyduk, Anal. Chem. 77 (2005) 1147–1156.
[8] Y. Lu, X.C. Li, L.M. Zhang, P. Yu, L. Su, L.Q. Mao, Anal. Chem. 80 (2008) 1883–1890.
[9] Y. Kang, K.J. Feng, J.W. Chen, J.H. Jiang, G.L. Shen, R.Q. Yu, Bioelectrochem 73 (2008) 76–81.
[10] W. Yao, L. Wang, H.Y. Wang, X.L. Zang, L. Li, Biosens. Bioelectron. 24 (2009) 3269–3274.
[11] Z. Zhelev, R. Bakalova, H. Ohba, R. Jose, Y. Imai, Y. Baba, Anal. Chem. 78 (2006) 321–330.
[12] T. Jin, F. Fujii, E. Yamada, Y. Nodasaka, M.J. Kinjo, J. Am. Chem. Soc. 128 (2006) 9288–9289.
[13] J.H. Choi, K.H. Chen, M.S. Strano, J. Am. Chem. Soc. 128 (2006) 15584–15585.
[14] C.L. Feng, X.H. Zhong, M. Steinhart, A.M. Caminade, J.P. Majoral, W. Knoll, Adv. Mater. 19 (2007) 1933–1936.

[15] S. Guo, E. Wang, Anal. Chim. Acta 598 (2007) 181–192.
[16] Y. Wang, W.P. Qian, Y. Tan, S.H. Ding, H.Q. Zhang, Talanta 72 (2007) 1134–1140.
[17] B. Ballarin, M.C. Cassani, E. Scavetta, D. Tonelli, Electrochim. Acta 53 (2008) 8034–8044.
[18] K.J. Huang, S. Yu, J. Li, Z.W. Wu, C.Y. Wei, Microchim. Acta 176 (2012) 327–335.
[19] K.J. Huang, J. Li, Y.M. Liu, X.Y. Cao, S. Yu, M. Yu, Microchim. Acta 177 (2012) 419–426.
[20] K.X. Mao, D. Wu, Y. Li, H.M. Ma, Z.Z. Ni, H.Q. Yu, C.N. Luo, Q. Wei, B. Du, Anal. Biochem. 422 (2012) 22–27.
[21] V. Singh, D. Joung, L. Zhai, S. Das, S.I. Khondaker, S. Seal, Prog. Mater. Sci. 56 (2011) 1178–1271.
[22] C.Z. Zhu, J.F. Zhai, D. Wen, S.J. Dong, J. Mater. Chem. 22 (2012) 6300–6306.
[23] K.J. Huang, D.J. Niu, X. Liu, Z.W. Wu, Y. Fan, Y.F. Chang, Y.Y. Wu, Electrochim. Acta 56 (2011) 2947–2953.
[24] Z. Yin, S. Sun, T. Salim, S. Wu, X. Huang, Q. He, Y.M. Lam, H. Zhang, ACS Nano 4 (2010) 5263–5268.
[25] M.A. Aziz, S. Patra, H. Yang, Chem. Commun. 38 (2008) 4607–4609.
[26] X.A. Zhang, J.F. Wang, W.J. Wu, S.W. Qian, Y.H. Man, Electrochem. Commun. 9 (2007) 2098–2104.